JOURNAL OF BIOMEDICAL OPTICS 4(1), 144–151 (JANUARY 1999)

DISPERSION EFFECTS IN PARTIAL COHERENCE INTERFEROMETRY: IMPLICATIONS FOR INTRAOCULAR RANGING

Christoph K. Hitzenberger, Angela Baumgartner, Wolfgang Drexler, and Adolf F. Fercher

University of Vienna, Institute of Medical Physics, Währinger Strasse 13, A-1090 Vienna, Austria

(Paper CDO-006 received Nov. 7, 1997; revised manuscript received Nov. 10, 1998; accepted for publication Nov. 10, 1998.)

ABSTRACT

In nondispersive media, the minimum distance that can be resolved by partial coherence interferometry (PCI) and optical coherence tomography (OCT) is inversely proportional to the source spectral bandwidth. Dispersion tends to increase the signal width and to degrade the resolution. We analyze the situation for PCI ranging and OCT imaging of ocular structures. It can be shown that for each ocular segment an optimum source bandwidth yielding optimum resolution exists. If the resolution is to be improved beyond this point, the group dispersion of the ocular media has to be compensated. With the use of a dispersion compensating element, and employing a broadband superluminescent diode, we demonstrate a resolution of 5 μm in the retina of both a model eye and a human eye *in vivo*. This is an improvement by a factor of 2–3 as compared to currently used instruments. © *1999 Society of Photo-Optical Instrumentation Engineers.* [S1083-3668(99)00701-7]

Keywords partial coherence interferometry; optical coherence tomography; dispersion; dispersion compensation; eye; ocular media.

1 INTRODUCTION

In the last decade, a new optical ranging technique, partial coherence interferometry (PCI), has been developed and applied to measure distances in biological objects, especially in the eye.[1–5] This technique was extended to optical coherence tomography (OCT), a new imaging modality capable of obtaining two-dimensional optical cross sections of the human retina with unprecedented axial resolution.[6–9]

The axial resolution of these techniques is approximately equal to the coherence length of the light source used. The coherence length l_c is inversely proportional to the width of the emission spectrum of the light source.[10] Presently used super luminescent diodes (SLDs) have a spectral width $\Delta\lambda \sim 25$ nm full width at half maximum (FWHM) at a center wavelength $\lambda_0 \cong 830$ nm. With these SLDs, a coherence length of ~ 13 μm in air is obtained. To improve the resolution of these techniques, strong efforts towards using light sources with broader emission spectra are in progress. With the use of broadband Ti:Al_2O_3 sources, resolution figures on the order of 2–4 μm (in air) were demonstrated.[11,12] These sources were applied to PCI ranging and OCT imaging of biologic samples of a total thickness of a few hundred micrometers.

Probably, the most important field of OCT application at present is imaging of the retina of the human eye.[7,13] In this case, the measured object, the retina, is located at the rear of a comparatively large body of dispersive material through which the measurements and the imaging have to be carried out. Dispersion tends to increase the width of the coherence envelope of the PCI scans which causes a decrease of the resolution and of the fringe visibility.[14–17] It is the purpose of this paper to evaluate these dispersion effects for the case of intraocular ranging. Based on properties of existing light sources and on the dispersion data of the ocular media,[17–19] we calculate the dispersion induced signal broadening and fringe visibility reduction for measurements in different ocular segments and recommend optimum light sources. For the most important case of ranging and imaging of the retina through the ocular media, we compare the calculated results with measurements obtained in a model eye. Furthermore, we show how the resolution can be improved by employing a special broadband SLD with $\Delta\lambda \cong 60$ nm in conjunction with compensating the group dispersion of the measured object, i.e., the ocular media. We demonstrate the improved resolution in a model eye and in a human eye *in vivo*.

Address all correspondence to Christoph K. Hitzenberger. Tel: (+43-1) 42 77 60711; Fax: (+43-1) 4277 9607; E-mail: christoph.hitzenberger@univie.ac.at

2 THEORETICAL ASPECTS

To measure distances by PCI and OCT, the object under investigation is placed in the measuring arm of a Michelson interferometer which is illuminated by a light source with high spatial coherence but short coherence length l_c. The length of the reference arm is scanned by a mirror and interferometric modulation is observed only if the (optical) path length of the reference arm is equal, within l_c, to that of the measuring arm. In this way reflection sites within the sample can be located with an axial resolution on the order of l_c. We define l_c as the roundtrip FWHM of the coherence envelope of an interferometric signal obtained from a specimen consisting of a single reflecting surface (a mirror). If the emission spectrum of the light source has a Gaussian shape and dispersion effects are neglected, l_c can be calculated by the following equation:[12]

$$l_c = \frac{2\ln(2)}{\pi}\frac{\lambda_0^2}{\Delta\lambda}, \tag{1}$$

where λ_0 is the center wavelength of the source and $\Delta\lambda$ is its FWHM spectral width.

If the object consists of a dispersive medium, i.e., the refractive index n of the medium depends on the wavelength, the different spectral components of a broadband light beam travel with different speed through the medium. In this case the wave groups emitted by the broadband source travel with the group velocity $v_g = c/n_g$ (c, vacuum light speed; n_g, group index) through the medium.[10] That means, the group index has to be used to relate the measured optical distances L_0 to the geometric distances L_g:[2,20,21] $L_0 = n_g L_g$. The group index n_g can be calculated from the refractive index n and the dispersion $dn/d\lambda$ by[22]

$$n_g = n - \lambda\frac{dn}{d\lambda}. \tag{2}$$

In a real material, the group index itself is a function of wavelength, i.e., a real material usually has a nonvanishing group dispersion (GD):

$$\mathrm{GD} = \frac{dn_g}{d\lambda} = -\lambda\frac{d^2n}{d\lambda^2}. \tag{3}$$

In a medium with group dispersion GD, the width of the coherence envelope increases, after double passing the medium with length L_g, to a value $l_{c,m}$ which can be calculated in the same way as the broadening of short light pulses in fiber optics:[22]

$$l_{c,m} = \sqrt{l_c^2 + (\mathrm{GD}\ L_g\Delta\lambda)^2}. \tag{4}$$

In Eq. (4), a Gaussian shape of the source spectrum is assumed. Furthermore, it is assumed that GD is constant within the range $\Delta\lambda$ and that the effects of higher order derivatives of the refractive index can be neglected.

For a given group dispersion, medium length, and center wavelength, an optimum source spectral width $\Delta\lambda_{\mathrm{opt}}$ yielding a minimum coherence length $l_{c,m}$ can be calculated. The condition $dl_{c,m}/d\Delta\lambda = 0$ yields

$$\Delta\lambda_{\mathrm{opt}} = \lambda_0\sqrt{\frac{2\ln(2)}{\mathrm{GD}\ L_g\pi}}. \tag{5}$$

A direct consequence of the dispersion broadening of the interferogram is a reduction of the interference fringe contrast or fringe visibility V. V is a function of the group delay τ between the interfering beams and is proportional to the modulus of the complex degree of coherence $|\gamma(\tau)|$.[10] It can be shown[23] that

$$\int_{-\infty}^{\infty} |\gamma(\tau)|^2\, d\tau = \mathrm{const}, \tag{6}$$

and, since $V(\tau) \propto |\gamma(\tau)|$ and the optical path difference $s = \tau \cdot v_g$:

$$\int_{-\infty}^{\infty} V(s)^2\, ds = \mathrm{const}. \tag{7}$$

That means that the effect of dispersion is to spread $V(s)^2$ over a greater range of optical path difference. If we assume a Gaussian shape of the coherence envelope and neglect higher order derivatives of GD, the overall shape of the coherence envelope, after double passing the medium, remains Gaussian,[15] however, with a change in width and height. Therefore, it follows from Eq. (7) that

$$V(s)^2 s_{\mathrm{FWHM}} = \mathrm{const}, \tag{8}$$

where s_{FWHM} is the FWHM width of the Gaussian function. If we take $s_{\mathrm{FWHM}} = l_c$ and $l_{c,m}$ for the cases before and after double passing the dispersive medium, respectively, we can calculate the maximum fringe visibility after double passing the medium, $V_{\mathrm{max},m}$, from the nondispersive value obtained in air, $V_{\mathrm{max,air}}$, by

$$V_{\mathrm{max},m} = V_{\mathrm{max,air}}\sqrt{\frac{l_c}{l_{c,m}}}. \tag{9}$$

That means that the signal amplitude of PCI and OCT is reduced by the same factor $\sqrt{l_c/l_{c,m}}$, if no countermeasures are taken.

To obtain the optimum resolution theoretically possible with broadband light sources and to avoid the reduction of fringe visibility, the dispersion of the object has to be compensated. This can be achieved by inserting a dispersion compensating el-

ement into the reference arm of the Michelson interferometer. This element must fulfill the condition:

$$GD_{el}L_{g,el} = GD_{ob}L_{g,ob}, \quad (10)$$

where the indices el and ob refer to the compensating element and the object, respectively.

3 METHODS

3.1 PARTIAL COHERENCE INTERFEROMETER

For PCI ranging of intraocular distances, we used a special ''dual beam'' partial coherence interferometer, as depicted in Figure 1. Details of the instrument have been described in earlier papers.[2,3,8,9] The main difference to other OCT systems using a ''classical'' interferometric setup is that the measured object, the eye, is not part of the Michelson interferometer. Instead, an external Michelson interferometer is used which splits the illuminating beam into two coaxial components that have a path difference of twice the interferometer arm length difference d. This dual beam illuminates the eye and is reflected at several intraocular interfaces. Thereby, each beam component of the dual beam is split into subcomponents having additional mutual phase delays. The reflected beam components are superimposed on the photodetector.

To measure intraocular distances, one of the interferometer mirrors is shifted and thereby d is altered. If d is equal (to within the coherence length) to one of the optical path differences within the eye, two of the several beam components remitted from the eye travel over the same total optical path length and hence interferometric modulation occurs at the detector. The envelope of the detector signal is recorded. The distance readout is performed with a cursor on a computer monitor. The resolution of this distance readout is 0.5 μm.

For practical reasons, all intraocular distances are measured to the anterior corneal surface as a reference surface. The advantage of this system is the complete elimination of artifacts caused by axial eye motions. Since only path differences are matched, the distance between instrument and eye is not important. For dispersion compensation with this dual beam PCI system, the dispersion compensating element has to be placed in the longer arm of the external Michelson interferometer, as indicated in Figure 1.

3.2 LIGHT SOURCES

As a light source, we used a special broadband infrared SLD (SLD 370, Superlum, Moscow: $\lambda_0 = 800\,\text{nm}$, $\Delta\lambda = 61\,\text{nm}$) with a maximum output power of 2 mW. The divergent beam was collimated by a special objective lens coated for near-infrared radiation (Nachet PL.FL 40×, France). The FWHM beam diameter at the position of the object (entrance of the eye) was approximately 0.7 mm.

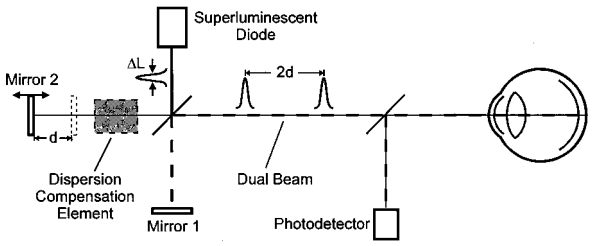

Fig. 1 Schematic diagram of dual beam partial coherence interferometer.

Figure 2(a) shows the emission spectrum of this SLD at 130 mA operating current. The spectrum was recorded with a Cynosure LS-2 spectrometer (Polytec, Waldbronn, Germany). The non-Gaussian, double-humped shape of the spectrum is caused by the internal structure of the SLD 370. According to the manufacturer, the SLD chip consists of two sections emitting at different central wavelengths. Figure 2(b) shows the coherence envelope obtained in air with the SLD 370 (solid line). It was measured by placing a mirror at the position of the object (cf. Figure 1). The dispersion compensating element of Figure 1 was removed in this case. The FWHM of the signal is $\cong 6\ \mu$m which is slightly larger than the value of $\Delta\lambda$ calculated by Eq. (1) (4.6 μm). The

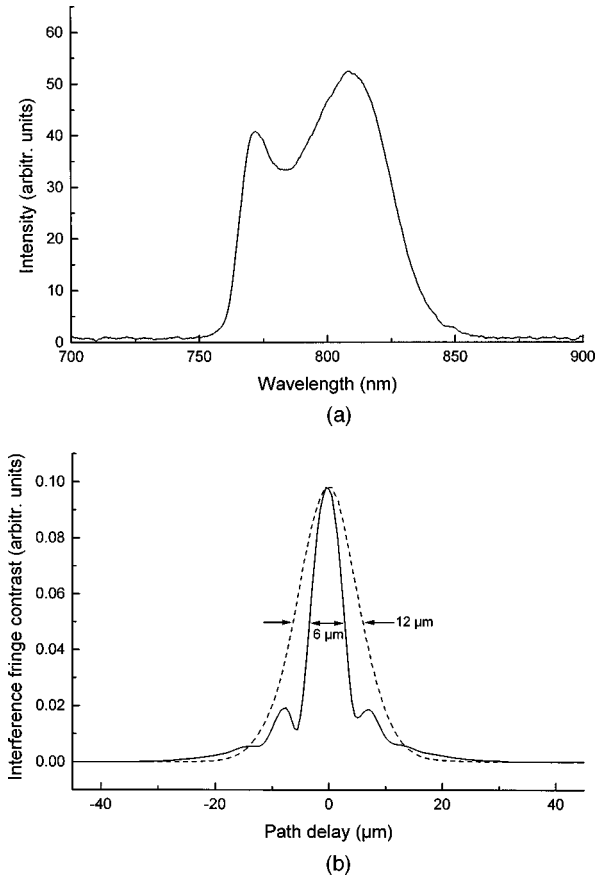

Fig. 2 (a) Emission spectrum of broadband SLD 370; (b) coherence envelope of SLD 370 (solid line) and of standard SLD (dashed line). The signals are normalized to equal amplitude.

Table 1 Group dispersion of different ocular media and of water (Refs. 17 and 19).

Medium	$dn_g/d\lambda$ (nm^{-1})
Cornea	$(-8.8\pm5.0)\times10^{-5}$
Aqueous	$(-1.43\pm1.05)\times10^{-5}$
Lens	$(-3.08\pm0.46)\times10^{-5}$
Average	$(-1.83\pm0.32)\times10^{-5}$
Water	-1.66×10^{-5}

reason might be the deviation from the Gaussian emission profile, on which Eq. (1) is based.

For comparison purposes, the coherence envelope of a standard SLD (EG&G C86142E, $\lambda_0 \cong 830$ nm, $\Delta\lambda = 26$ nm) is also shown in Figure 2(b) (dashed line). Its FWHM is 12 μm, very close to the theoretical value of 11.7 μm (the emission profile of this diode has nearly Gaussian shape).

3.3 DATA FOR THEORETICAL CALCULATIONS

3.3.1 Light Sources

In addition to the standard SLD and the broadband SLD mentioned above, two other light sources were evaluated by theoretical calculations: (i) a combined source consisting of two spectrally displaced SLDs with $\lambda_{01}=830$ nm and $\lambda_{02}=856$ nm. Due to a beat effect, this combined source behaves similar to a single source with center wavelength $\lambda_{0,\mathrm{eff}}=843$ nm and $\Delta\lambda_{\mathrm{eff}}=50$ nm;[17,18,24,25] (ii) a very wide band Ti:Al_2O_3 source with $\lambda_0=820$ nm and $\Delta\lambda \cong 140$ nm. Although the emission spectrum of these sources is non-Gaussian, a Gaussian shape was assumed to simplify the calculations.

3.3.2 Group Dispersion of Ocular Media

We recently measured the group dispersion of the ocular media in the near-infrared range.[17–19] This was done by measuring the intraocular optical distances with two different SLDs with center wavelengths of 814 and 855 nm, respectively. From the shift of the signal peaks, the group dispersion of cornea, aqueous, lens, as well as a mean value of the GD, averaged over the whole axial eye length, was determined. For comparison purposes, the GD of water was also measured. The results are shown in Table 1.

4 RESULTS

4.1 CALCULATION OF DISPERSION BROADENING

To estimate the effect of dispersion broadening in intraocular ranging, different cases were considered: Corneal thickness measurements, measurements within the anterior eye segment (i.e., up to the posterior lens surface), and measurements of the whole axial eye length or within the retina (through all of the ocular media). To simplify the calculations, an effective water length L_{eff} was calculated for each case. This is the geometric path length in water causing the same group dispersive effect as the respective medium of length L_g. This effective length is based on Gullstrands schematic eye[26] and on the group dispersion of water for $\lambda = 830$ nm (cf. Table 1):

$$L_{\mathrm{eff}} = L_{g,\mathrm{medium}} \frac{\mathrm{GD}_{\mathrm{medium}}}{\mathrm{GD}_{\mathrm{water}}}. \tag{11}$$

The coherence length of a light beam in air (without dispersion) was calculated using Eq. (1), that of the beam after double passing a dispersive medium of length L_g by using Eq. (4). The maximum fringe visibility was calculated by Eq. (9), assuming $V_{\mathrm{max,air}}=1$. The calculations were performed for the four different light sources mentioned in the materials section using the effective water lengths of Table 2 and the group dispersion of water.[27] Table 2 summarizes the results. It is clearly shown that the resolution of measurements within the retina dramatically degrades if a light source with larger spectral bandwidth than that of a single SLD is used. Furthermore, the fringe visibility is reduced considerably.

If the dispersion of the ocular media is not compensated, there is an optimum source bandwidth yielding optimum resolution. This optimum bandwidth is different for the different ocular segments and can be calculated by Eq. (5). Assuming a center wavelength of $\lambda_0=830$ nm, the effective water lengths of Table 2, and the group dispersion of water at $\lambda=830$ nm (cf. Table 1), we calculated the optimum source bandwidths and the corresponding optimum resolution figures for ranging in the different ocular segments. The results are shown in Table 3.

4.2 EXPERIMENTAL RESULTS

To demonstrate the dispersive effects expected from measurements in the ocular fundus, a model eye (Eyetech Ltd., IL) was used as the object. This model eye consists of a ''cornea'' made of acryl glass and a body filled with water. Different reflectors can be inserted at the ''fundus'' of the eye resembling the ''retina.'' The geometric distance between the cornea and the retina was about 25.8 mm. At first, a single reflective interface (a mirror) was used as the retina. Figure 3(a) shows the signal obtained without dispersion compensation. The solid line shows the coherence envelope recorded with the broadband SLD 370. The double hump, asymmetric shape of this coherence envelope is caused by the corresponding asymmetric shape of the emission spectrum. The FWHM of the signal is

Table 2 Calculated values of dispersion broadening and fringe visibility reduction for different ocular segments and light sources. l_c, coherence length in air; $l_{c,m}$, coherence length after double passing the ocular segment; $V_{max,m}$, fringe visibility maximum after double passing the ocular segment, if $V_{max,air}=1$ is assumed.

		Single SLD	Two SLDs	Broadband SLD	Ti:Al_2O_3
	Effective water	$\lambda_0=830$ nm	$\lambda_{0,eff}=843$ nm	$\lambda_0=800$ nm	$\lambda_0=820$ nm
Ocular segment	length L_{eff}	$\Delta\lambda=26$ nm	$\Delta\lambda_{eff}=50$ nm	$\Delta\lambda=61$ nm	$\Delta\lambda=140$ nm
Air (no dispersion)	0 mm	$l_c=11.7\ \mu$m	$l_c=6.3\ \mu$m	$l_c=4.6\ \mu$m	$l_c=2.1\ \mu$m
		$V_{max,m}=1$	$V_{max,m}=1$	$V_{max,m}=1$	$V_{max,m}=1$
Cornea	2.65 mm	$l_{c,m}=11.7\ \mu$m	$l_{c,m}=6.6\ \mu$m	$l_{c,m}=5.7\ \mu$m	$l_{c,m}=6.9\ \mu$m
		$V_{max,m}=1$	$V_{max,m}=0.98$	$V_{max,m}=0.90$	$V_{max,m}=0.55$
Anterior segment	12.4 mm	$l_{c,m}=12.9\ \mu$m	$l_{c,m}=11.3\ \mu$m	$l_{c,m}=16.2\ \mu$m	$l_{c,m}=31.0\ \mu$m
		$V_{max,m}=0.95$	$V_{max,m}=0.75$	$V_{max,m}=0.53$	$V_{max,m}=0.26$
Axial eye length,	26.5 mm	$l_{c,m}=16.4\ \mu$m	$l_{c,m}=21.0\ \mu$m	$l_{c,m}=33.5\ \mu$m	$l_{c,m}=66.1\ \mu$m
posterior segment		$V_{max,m}=0.84$	$V_{max,m}=0.55$	$V_{max,m}=0.37$	$V_{max,m}=0.18$

$\sim 40\ \mu$m, which is somewhat more than the calculated value of 33.5 μm (cf. Table 2), probably because of the non-Gaussian shape of the emission spectrum. It is obvious that this signal is not suited for high resolution measurements. The dashed line shows the signal obtained with the standard SLD. It is only moderately broadened.

To improve the situation, a dispersion compensating element was inserted in the longer arm of the external Michelson interferometer (cf. Figure 1). We used a plane parallel BK7 glass plate of $L_{el}=12$ mm. This material has a GD of 3.46×10^{-5}/nm at $\lambda_0=830$ nm[28] and compensates about 23.3 mm of water, i.e., only ~ 2 mm of water is not compensated. Figure 3(b) shows the result of a measurement in the model eye obtained with dispersion compensation. The signal shape obtained with the SLD 370 (solid line) is now almost symmetric and the FWHM of the signal is 6.5 μm, which indicates almost perfect dispersion compensation. This signal resembles the point spread function (PSF) of the compensated system. The dashed line shows the signal recorded with the standard SLD. After dispersion compensation, the broadband SLD obtains an approximately twofold better resolution than the standard SLD.

To demonstrate the resolution of two closely spaced surfaces, we replaced the mirror in the model eye by a transparent polyethylen–terephthalat (PET) foil with 4 μm thickness. Figure 4 shows a PCI scan obtained from this foil with the SLD 370 and dispersion compensation. Two signal peaks at a distance of $\sim 7\ \mu$m are observed. Assuming a refractive index of 1.6 (according to the manufacturer), the foil thickness is measured to be 4.4 μm, which is very close to the nominal value of 4 μm (the resolution of the distance readout of our system is 0.5 μm).

Finally, we performed a measurement in a human eye *in vivo*. Again, the SLD 370 was used. The

Table 3 Optimum source bandwidth and optimum resolution calculated for PCI ranging and OCT imaging in different ocular segments. For the calculation of the geometrical distance, a mean group refractive index of 1.355 was assumed (Ref. 2).

Ocular segment	Eff. water length	Optimum source bandwidth	Optimum resol. (opt. dist.)	Optimum resol. (geom. dist.)
Cornea	2.65 mm	83 nm	5.2 μm	3.8 μm
Anterior segment	12.4 mm	38 nm	11.2 μm	8.3 μm
Axial eye length, posterior segment	26.5 mm	26 nm	16.4 μm	12.1 μm
Posterior segment compensated to ± 3 mm effective water length	3 mm	78 nm	5.5 μm	4.1 μm

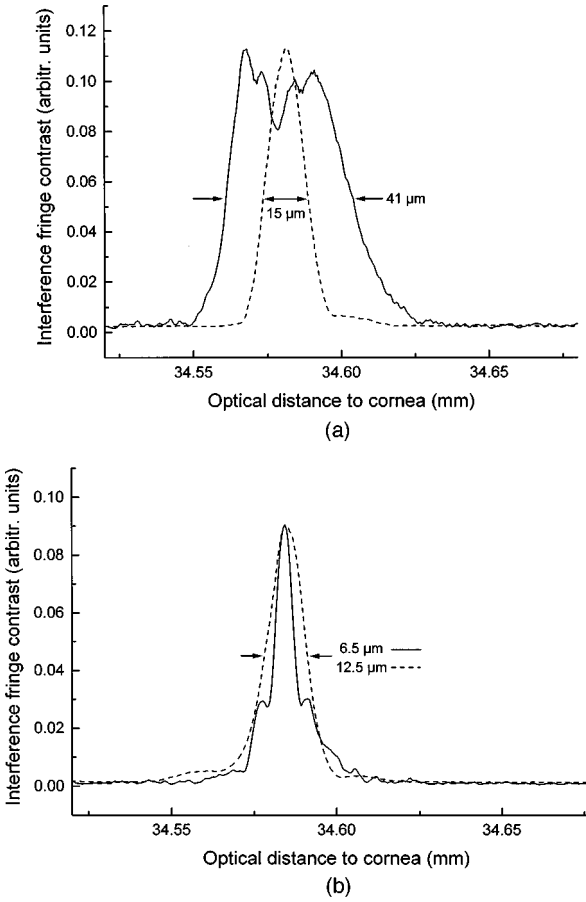

Fig. 3 PCI signals obtained from the ''fundus'' of a model eye with a mirror at the position of the ''retina.'' Solid line: signal obtained with broadband SLD 370; dashed line: signal obtained with standard SLD. The signals are normalized to equal amplitude; (a) without and (b) with dispersion compensation. The two SLDs have different center wavelengths, therefore there is a small dispersion induced shift between the signals. For easy comparison, the signal obtained with the standard SLD was centered with respect to that of the SLD 370.

measurement was performed in the left eye of a healthy volunteer, after informed consent was obtained. A single PCI scan was performed at 5° nasal. The eye was illuminated by a beam of $\sim 150\,\mu$W power or 390 μW/cm^2 averaged over a 7 mm aperture. Alignment and measurement procedure took less than 1 min, which is far below the safety limits.[29] Figure 5 shows the result. Several narrow signal peaks are observed. The peak at ~ 33.7 mm indicates the position of the inner limiting membrane. Its shape is very similar to that of the PSF of the system [Figure 3(b)]. This indicates the proper alignment of a diffractive optical element in front of the cornea which is used to improve the signal to noise ratio[9,30] (misalignments might cause signal distortions). The peaks at ~ 34.1 mm indicate structures at the posterior boundary of the retina. The width of the signal peaks is $\sim 7\,\mu$m, which indicates a geometric resolution of $\sim 5\,\mu$m within the retina, if a group index of ~ 1.4 is assumed.

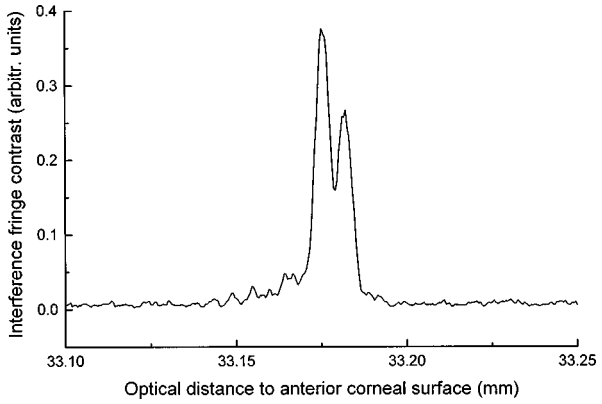

Fig. 4 Dispersion compensated PCI signal obtained from the ''fundus'' of a model eye with the broadband SLD 370. The ''retina'' consists of a 4-μm-thick transparent PET foil.

5 DISCUSSION

It is well known that for certain types of interferometric measurements the two arms of an interferometer have to be dispersion balanced. The problem of dispersion induced signal broadening in PCI was first discussed in the context of fiber and waveguide optics.[14,16] In the field of biomedical optics, high resolution PCI and OCT employing light sources with a bandwidth larger than that of standard SLDs were yet used only for ranging and imaging within tissues with a thickness of a few hundred μm.[11,12] In this case the dispersive effects of the object can be neglected.

We have evaluated the effects of group dispersion in the case of intraocular ranging and imaging. We have demonstrated, both by theoretical calculations and experimental measurements, that in this case the group dispersion of the object, i.e., the ocular media, is the factor that limits the resolution of

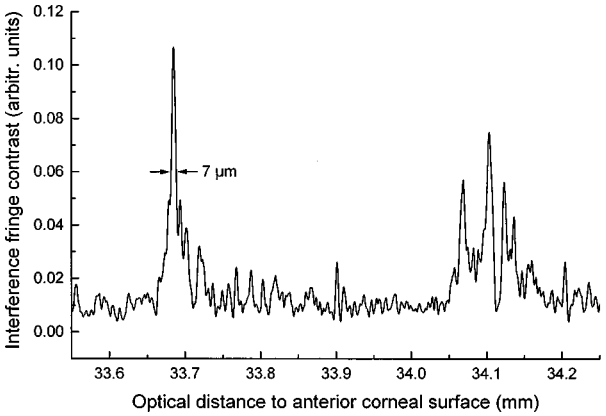

Fig. 5 Dispersion compensated PCI signal obtained from the fundus of a human eye *in vivo* with the broadband SLD 370. The signal width of 7 μm corresponds to a geometric resolution of 5 μm in the medium.

PCI and OCT. If the dispersion of the ocular media is not compensated, the optimum wavelength for ranging and imaging in the anterior segment of the eye is ~40 nm. An appropriate source could be a combination of two spectrally displaced SLDs. However, the optimum resolution would be not better than ~11 μm optical distance or ~8 μm geometrical distance (cf. Table 3).

Presently the most important field of OCT is imaging of the retina of the human eye. In this case, the measurements have to be performed through the whole length of the dispersive ocular media. Without dispersion compensation, the optimum source bandwidth for retinal imaging is ~26 nm, i.e., that of a standard SLD. The resolution is ~16 μm optical distance or ~12 μm geometrical distance in this case. If a wider bandwidth is used, the resolution is not improved but degraded. Furthermore, the fringe contrast and therefore the signal-to-noise ratio is reduced.

If the dispersion of the ocular media is compensated, the situation can be improved considerably. By using a SLD with $\Delta\lambda = 61$ nm and a dispersion compensating element made of BK7 glass, we have demonstrated an axial resolution of $\cong 7$ μm optical distance or $\cong 5$ μm geometrical distance in the retina of both a model eye and a human eye *in vivo*. This is an improvement by a factor of about 2–3 compared to previously reported resolution figures within the retina. It is obvious that the same technique can be used to improve depth resolution in OCT as well.

If a dispersion compensating element of fixed length is used, it should be chosen to compensate the dispersion of ''standard eyes'' of ~24 mm length (corresponding to ~26.5 μm effective water length). Individual eyes differ from this standard length usually not by more than 3 mm, if extreme cases of myopia are neglected. Therefore, a dispersion compensation to within ± 3 mm of effective water length can be assumed. The optimum light source for this case would have a bandwidth of $\Delta\lambda_{opt} = 78$ nm (cf. Table 3). This could be a combination of two or three SLDs or a broadband SLD. The optimum resolution would be $\cong 5.5$ μm optical distance or $\cong 4$ μm geometrical distance. To exploit the possible resolution of ~2 μm of a very wide band Ti:Al_2O_3 source, each eye would require an individual dispersion compensation adapted to its length. If not only the area of the retina but the entire length of the eyeball was scanned, a dynamic dispersion compensation would have to be used.

Acknowledgments

The authors thank Mr. H. Sattmann for excellent technical assistance. Financial assistance from the Austrian ''Fonds zur Förderung der wissenschaftlichen Forschung'' (FWF Grant P9781-MED) is acknowledged.

REFERENCES

1. A. F. Fercher and E. Roth, ''Ophthalmic laser interferometry,'' *Proc. SPIE* **658**, 48–51 (1986).
2. C. K. Hitzenberger, ''Optical measurement of the axial eye length by laser Doppler interferometry,'' *Invest. Ophthalmol. Visual Sci.* **32**, 616–624 (1991).
3. C. K. Hitzenberger, ''Measurement of corneal thickness by low-coherence interferometry,'' *Appl. Opt.* **31**, 6637–6642 (1992).
4. W. Drexler, A. Baumgartner, O. Findl, C. K. Hitzenberger, H. Sattmann, and A. F. Fercher, *Invest. Ophthalmol. Visual Sci.* **38**, 1304–1313 (1997).
5. G. F. Schmid, B. L. Petrig, C. E. Riva, K. H. Shin, R. A. Stone, M. J. Mendel, and A. M. Laties, ''Measurement by laser Doppler interferometry of intraocular distances in humans and chicks with a precision of better than ± 20 μm,'' *Appl. Opt.* **35**, 3358–3361 (1996).
6. D. Huang, E. A. Swanson, C. P. Lin, J. S. Schuman, W. G. Stinson, W. Chang, M. R. Hee, T. Flotte, K. Gregory, C. A. Puliafito, and J. G. Fujimoto, ''Optical coherence tomography,'' *Science* **254**, 1178–1181 (1991).
7. M. R. Hee, J. A. Izatt, E. A. Swanson, D. Huang, J. S. Schuman, C. P. Lin, C. A. Puliafito, and J. G. Fujimoto, ''Optical coherence tomography of the human retina,'' *Arch. Opthalmol. (Chicago)* **113**, 325–332 (1995).
8. A. F. Fercher, ''Optical coherence tomography,'' *J. Biomed. Opt.* **1**, 157–173 (1996).
9. A. Baumgartner, B. Möller, C. K. Hitzenberger, W. Drexler, and A. F. Fercher, ''Measurement of the posterior structures of the human eye *in vivo* by partial coherence interferometry using diffractive optics,'' *Proc. SPIE* **2981**, 85–93 (1997).
10. M. Born and E. Wolf, *Principles of Optics*, 6th ed., Pergamon, Oxford (1987).
11. X. Clivaz, F. Marquis-Weible, and R.-P. Salathé, ''1.5 μm resolution optical low coherence reflectometry in biological tissues,'' *Proc. SPIE* **2083**, 338–346 (1994).
12. B. Bouma, G. J. Tearney, S. A. Boppart, M. R. Hee, M. E. Brezinski, and J. G. Fujimoto, ''High-resolution optical coherence tomographic imaging using a mode-locked Ti:Al_2O_3 laser source,'' *Opt. Lett.* **20**, 1486–1488 (1995).
13. C. A. Puliafito, M. R. Hee, C. P. Lin, E. Reichel, J. S. Schuman, J. S. Duker, J. A. Izatt, E. A. Swanson, and J. G. Fujimoto, ''Imaging of macular diseases with optical coherence tomography,'' *Ophthalmology (Philadelphia)* **102**, 217–229 (1995).
14. E. Brinkmeyer and R. Ulrich, ''High-resolution OCDR in dispersive waveguides,'' *Electron. Lett.* **26**, 413–414 (1990).
15. B. L. Danielson and C. Y. Boisrobert, ''Absolute optical ranging using low coherence interferometry,'' *Appl. Opt.* **30**, 2975–2979 (1991).
16. A. Kohlhaas, C. Frömchen, and E. Brinkmeyer, ''High-resolution OCDR for testing integrated-optical waveguides: Dispersion-corrupted experimental data corrected by a numerical algorithm,'' *J. Lightwave Technol.* **9**, 1493–1502 (1991).
17. C. K. Hitzenberger, W. Drexler, A. Baumgartner, and A. F. Fercher, ''Dispersion effects in partial coherence interferometry,'' *Proc. SPIE* **2981**, 29–36 (1997).
18. W. Drexler, C. K. Hitzenberger, A. Baumgartner, O. Findl, H. Sattmann, and A. F. Fercher, ''Multiple wavelength partial coherence interferometry,'' *Proc. SPIE* **2930**, 194–201 (1996).
19. W. Drexler, C. K. Hitzenberger, A. Baumgartner, O. Findl, H. Sattmann, and A. F. Fercher, ''Investigation of dispersion effects in ocular media by multiple wavelength partial coherence interferometry,'' *Exp. Eye Res.* **66**, 25–33 (1998).
20. S. Pancharatnam, ''Partial polarisation, partial coherence and their spectral description for polychromatic light-part II,'' *Proc.-Indian Acad. Sci., Sect. A* **57**, 231–243 (1963).
21. P. de Groot, ''Chromatic dispersion effects in coherent absolute ranging,'' *Opt. Lett.* **17**, 898–900 (1992).
22. E.-G. Neumann, *Single-Mode Fibers*, Chap. 11.5, Springer, Berlin (1988).
23. W. J. Tango, ''Dispersion in stellar interferometry,'' *Appl. Opt.* **29**, 516–521 (1990).
24. Y. J. Rao, Y. N. Ning, and D. A. Jackson, ''Synthesized

source for white-light sensing systems,'' *Opt. Lett.* **18**, 462–464 (1993).
25. D. N. Wang, Y. N. Ning, K. T. V. Grattan, A. W. Palmer, and K. Weir, ''Optimized multiwavelength combination sources for interferometric use,'' *Appl. Opt.* **33**, 7326–7333 (1994).
26. H. Obstfeld, *Optics in Vision*, pp. 28–42, Butterworth, London (1982).
27. M. Eckholt, Untersuchung der Messbarkeit der Dispersion mittels Spektralinterferometrie für die Stoffe Kronglas BK7, Schwerflintglas SF11, Wasser und Zinkselenid, Diploma thesis, pp. 35–36, Technical University of Vienna, 1995.
28. W. J. Tropf, M. Thomas, and T. J. Harris, ''Properties of crystals and glasses,'' in *Handbook of Optics*, M. Bass, E. W. Van Stryland, D. R. Williams, W. L. Wolfe, Eds., 2nd ed., Vol. II, Chap. 33, p. 33.67, McGraw-Hill, New York (1995).
29. American National Standards Institute, *Safe Use of Lasers*, ANSI Z 136.1, American National Standards Institute, New York (1986).
30. B. Möller, G. Rudolph, A. Klopffleisch, K. H. Donnerhacke, and A. Dorsel, ''Application of diffractive optics for axial eye length measurement using partial coherence interferometry,'' *Proc. SPIE* **2930**, 175–182 (1996).